AMERICAN SOCIETY FOR MICROBIOLOGY | Applied and Environmental Microbiology

Genomics and Proteomics | Full-Length Text

Comparative genomics of the niche-specific plant pathogen *Streptomyces ipomoeae* reveal novel genome content and organization

Natasha R. Soares,[1] José C. Huguet-Tapia,[2] Dongli Guan,[1] Christopher A. Clark,[3] Kuei-Ting Yang,[1] Olivia R. Kluchka,[1] Raju S. Thombal,[4] Rendy Kartika,[4] Jonathan H. Badger,[5] Gregg S. Pettis[1,3]

AUTHOR AFFILIATIONS See affiliation list on p. 18.

ABSTRACT The sweet potato soil rot pathogen *Streptomyces ipomoeae* differs in disease pathology, host range, and virulence factor production from *Streptomyces* species that cause scab diseases on potato and other plant hosts. Nevertheless, previous phylogenomic analysis suggested *S. ipomoeae* and the oldest scab species, *Streptomyces scabiei*, are derived from a common ancestor. While genomes of scab pathogens have been described in some detail, similar knowledge of *S. ipomoeae* has been lacking. Here, we performed comparative genomic analyses involving both virulent and avirulent strains of *S. ipomoeae,* along with other plant-pathogenic and saprophytic *Streptomyces* spp. The *txt* gene cluster for the phytotoxin thaxtomin C was found in all virulent strains of *S. ipomoeae*, but, contrary to scab species, the thaxtomin locus does not appear to reside within a genomic island and has diverged from its scab pathogen counterparts. Increased TTA rare codon usage appears to be a hallmark of *S. ipomoeae*, and in particular, for its *txt* locus. The *txtR* activator gene, which we show here is essential for pathogenicity, appears to be subject to exceptional *bldA* translational control. Ortholog group searches identified genes found only in virulent *S. ipomoeae* strains in our analysis, and genome mining revealed secondary metabolite gene clusters of *S. ipomoeae*, which are not shared with scab species. Overall, we have identified novel aspects of genome organization and gene content consistent with niche development by *S. ipomoeae*, and the results here will facilitate the elucidation of the mechanisms governing its virulence and ecology.

IMPORTANCE While most plant-pathogenic *Streptomyces* species cause scab disease on a variety of plant hosts, *Streptomyces ipomoeae* is the sole causative agent of soil rot disease of sweet potato and closely related plant species. Here, genome sequencing of virulent and avirulent *S. ipomoeae* strains coupled with comparative genomic analyses has identified genome content and organization features unique to this streptomycete plant pathogen. The results here will enable future research into the mechanisms used by *S. ipomoeae* to cause disease and to persist in its niche environment.

KEYWORDS thaxtomin, plant pathogens, *Streptomyces*

Research involving mycelial spore-forming *Streptomyces* bacteria tends to focus on industrially and pharmaceutically relevant secondary metabolite biosynthesis among members of this large and predominantly saprophytic genus. A rarer trait, which has received less attention, is the ability of a small number of species to cause disease on certain plant crops and model species. The most studied plant-pathogenic *Streptomyces* spp. are known as scab pathogens and they consist of nearly a dozen species, including the oldest known scab pathogen *Streptomyces scabiei*. They induce characteristic

Editor Isaac Cann, University of Illinois Urbana-Champaign, Urbana, Illinois, USA

Address correspondence to Gregg S. Pettis, gpettis@lsu.edu.

The authors declare no conflict of interest.

See the funding table on p. 18.

Received 22 February 2023
Accepted 28 September 2023

Published 27 November 2023

scab-like symptoms and are neither host nor tissue-specific but typically infect tuber and root crops such as potatoes, beets, carrots, parsnip, radishes, and many others (1). Scab symptoms include round, raised, moderately necrotic lesions sometimes with pitted centers (2). Scab pathogens target rapidly expanding tissue, a characteristic that appears to be facilitated by the production of the phytotoxin, thaxtomin A, a cellulose biosynthesis inhibitor (2).

Thaxtomin A is a dipeptide produced from a biosynthetic pathway encoded by the *txt* gene cluster (*txtA*, *txtB*, *txtC*, *txtD*, *txtE*, *txtH*, and *txtR*). The TxtD (nitric oxide synthase) and TxtE (P450-monooxygenase) proteins are responsible for nitrating tryptophan into 4-nitrotryptophan (3), while methylation and cyclization of 4-nitrotryptophan and L-phenylalanine are catalyzed by the TxtA and TxtB non-ribosomal peptide synthetase proteins (NRPSs) (4, 5). The TxtH protein, a member of the MbtH-like protein superfamily, promotes the proper folding of the TxtA and TxtB NRPSs (6). Post-cyclic hydroxylation of the thaxtomin dipeptide is then accomplished by the TxtC (P450 monooxygenase) protein (7). Thaxtomin gene knockout mutants of *Streptomyces* scab pathogens were found to be avirulent on potato tubers (4, 8).

Also encoded in the thaxtomin A gene cluster is an AraC/XylS family regulatory protein, TxtR, which is similarly required for pathogenicity (9). It was previously reported that the *txtR* gene of *S. scabiei* contains a single TTA codon (9). Since *Streptomyces* spp. have genomes with approximately 72% G + C content and show a substantial bias for G + C-rich codons, TTA codons are extremely rare in these organisms and single copies of TTA are typically found within genes responsible for secondary metabolism regulation and control of aerial hyphae development (10). Moreover, TTA codons are subject to regulation by the *bldA* gene, whose leucyl tRNA product is developmentally regulated and is the only cognate species for this codon (10, 11). Deletion of *bldA* in *S. scabiei* eliminated thaxtomin A production and virulence in radish seedlings (12).

The organization of virulence loci in the genomes of *Streptomyces* scab pathogens, including how some species carry virulence genes on pathogenicity islands (PAIs), has provided clues regarding the evolution of plant pathogenicity in the genus. Indeed, the ability of some PAIs to be conjugally transferred and to confer a pathogenic phenotype on certain saprophytic streptomycete recipients has been demonstrated experimentally in several studies (13–16).

In *S. scabiei*, two PAIs are located ~5 Mb apart at conserved loci. One PAI, the toxicogenic region (TR) (17), is inserted at a conserved attachment (*att*) site within the 3′ end of the *aviX1* gene, which encodes a putative ATP/GTP-binding protein. TR is composed of two modules—the 20-kb TR1 module, which contains the thaxtomin A gene cluster, and the 157-kb TR2 module, which contains genes responsible for excision, integration, and conjugation of TR (18). TR2 thus appears to fit the criteria of an integrative and conjugative element (ICE) (16). Recent experimental evidence suggests that TR1 is not an ICE but, upon integration of TR2 in *cis* next to TR1, the latter can be mobilized to transfer. Therefore, TR1 was classified as a cis-mobilizable element (CIME) (16).

The colonization region (CR) (17) is the other PAI in *S. scabiei,* and it is inserted at the 3′ end of the bacitracin resistance (*bacA*) gene. Included in the 105-kb CR is *nec1*, a gene that encodes a secreted necrogenic protein that appears to facilitate infection, and *tomA*, which encodes a functional tomatinase, a saponin-detoxifying enzyme that may play a role in the suppression of induced host defenses (19, 20). The potential for excision, integration, and conjugation of CR has not been investigated.

While the composite TR has been found consistently at *aviX1* in strains of *S. scabiei* (16), TR is not conserved in more recently emerged scab pathogens. *Streptomyces turgidiscabies* strain Car8 contains no island at *aviX1* but instead possesses a large 674-kb modular PAI (i.e., PAISt) at *bacA*, which includes the thaxtomin A biosynthetic genes, *nec1*, *tomA* and a fasciation (*fas*) operon homologous to the one found in the actinomycete plant pathogen *Rhodococcus fascians* (21). In *Streptomyces acidiscabies*, the configuration of TR at *aviX1* was found to differ greatly among strains with some

containing only TR1, one containing the full TR, and others lacking TR completely (16). Strains of another scab pathogen, *Streptomyces niveiscabiei*, also varied in their TR composition (16). Thus, TR can vary among more recently emerging scab pathogens, while it appears to be conserved in *S. scabiei*.

In contrast to common scab, soil rot is an intensely necrotic disease caused by a single species, *Streptomyces ipomoeae,* whose natural host range is restricted to members of the plant family Convolvulaceae (22). This pathogen can cause a great economic impact on sweet potato, *Ipomoea batatas* (L.) Lam., due to necrotic destruction of adventitious roots as well as deformations and lesions that develop on the fleshy edible storage roots (23).

S. ipomoeae also produces thaxtomin, but it is a less-modified, non-hydroxylated version known as thaxtomin C (24). Cloning and characterization of the thaxtomin C gene cluster from *S. ipomoeae* strain 91-03 revealed the presence of *txtA*, *txtB*, *txtD*, *txtE*, *txtH*, and *txtR* homologs in this species, but as expected, no *txtC* gene was present. Knockout of thaxtomin biosynthetic genes in *S. ipomoeae* 91-03 eliminated pathogenicity on intact sweet potato adventitious roots (25).

A further distinguishing feature of *S. ipomoeae* is an interstrain growth inhibition phenotype, which is apparent upon pairwise cultivation of strains on agar plates (26). It was found that most *S. ipomoeae* strains analyzed could be divided into three groups based on interstrain inhibition profiles. Group I strains did not inhibit members of the other groups, while group II strains inhibited group I and III strains, and likewise, group III strains inhibited group I and II strains (26). The group III interstrain inhibitor molecule was later identified as a bacteriocin (ipomicin), which is bacteriolytic and highly specific for group I and II *S. ipomoeae* strains. The structural gene for ipomicin, *ipoA*, was also cloned and sequenced from the group III strain 91-03 (27).

Despite the many phenotypic and genotypic differences noted, previous phylogenomic analysis supported the view that the soil rot pathogen *S. ipomoeae* and the scab pathogen *S. scabiei* are derived from a common ancestor (28). Divergence into separate species then occurred, perhaps driven by the development of a niche specificity for *S. ipomoeae*. Lateral gene transfer of pathogenicity islands from *S. scabiei* then fueled the emergence of additional scab species (28). While the genomes of *S. scabiei* and a number of other scab pathogen genomes have been described in some detail, similar knowledge of *S. ipomoeae* has been lacking. To gain insights regarding the latter, here we have performed comparative analyses involving both virulent and avirulent strains of *S. ipomoeae*, as well as other plant pathogenic and saprophytic *Streptomyces* genomes. Such analyses have clarified the content and organization of the *S. ipomoeae* genome, including identifying additional distinguishing features of thaxtomin production in this species as well as revealing other genes that may function in virulence and/or ecology of this unique streptomycete plant pathogen.

RESULTS AND DISCUSSION

Comparative genomic approach and description of draft sequences for *S. ipomoeae* strains 78-51, 88-35, and B12321

The 10.4-Mb draft sequence of the pathogenic *S. ipomoeae* strain 91-03 was included in the initial phylogenomic analysis of plant-pathogenic *Streptomyces* spp. (28). To gain more insight specifically into the soil rot pathogen genome, two additional pathogenic *S. ipomoeae* strains, namely 78-51 and 88-35, were sequenced, along with the original neotype strain B12321 (ATCC-25462). Following its isolation from diseased sweet potatoes (circa 1940s), strain B12321 has since become nonpathogenic, probably due to extended passaging in laboratories and lack of selective pressure for virulence (26, 29). Inclusion of B12321 in our comparative analyses will, therefore, aid in identifying genes found only in the pathogenic *S. ipomoeae* isolates, which may be important for the virulence and/or ecological persistence of the bacterium. Moreover, despite its avirulent phenotype, strain B12321 still colonizes sweet potato adventitious roots (K.-T. Yang, N. R. Soares, C. A. Clark, and G. S. Pettis, unpublished data); thus, characterization of the strain B12321 genome may facilitate its use in biocontrol applications. All genome sequences

TABLE 1 Genome sequences used in this study

Organism	Strain	Genome size (Mb)[a]	Reference or source	Genbank assembly accession no.
Streptomyces acidiscabies	84–104	11.0	(30)	GCA_000242715.2
S. acidiscabies	85–06	11.0	(16)	GCA_001941285.1
S. acidiscabies	98–48	10.6	(16)	GCA_001941275.1
S. acidiscabies	98–49	10.2	(16)	GCA_001941265.1
S. acidiscabies	FL01	10.6	(16)	GCA_001941325.1
S. acidiscabies	A10	10.7	(31)	GCA_001485105.1
S. acidiscabies	A2	10.6	Kagoshima Institute for Agricultural Development, Japan	GCA_001949645.1
S. acidiscabies	NCPPB-4445	10.0	University of Exeter	GCA_001189015.1
S. acidiscabies	ST105	10.8	Universidad de la República, Uruguay	GCA_003584805.1
Streptomyces albus	NRRL F-4971	6.9	(32)	GCA_000719865.1
Streptomyces avermitilis	MA-4680	9.1*	(33)	GCA_000009765.2
Streptomyces bingchenggensis	BCW-1	11.9*	(34)	GCA_000092385.1
Streptomyces cattleya	DSM 46488	8.1*	Shanghai Jiaotong University	GCA_000240165.1
Streptomyces coelicolor	A3(2)	9.1*	(35)	GCA_000203835.1
Streptomyces diastatochromogenes	NRRL B-1698	9.1	(36)	GCA_001418405.1
Streptomyces europaeiscabiei	89–04	10.5	(14)	GCA_001550325.1
S. europaeiscabiei	96–14	10.5	(14)	GCA_001550375.1
S. europaeiscabiei	NCPPB 4064	8.6	University of Exeter	GCA_001189025.1
S. europaeiscabiei	NRRL B-24443	10.0	USDA/ARS/NCAUR	GCA_000988945.1
S. europaeiscabiei	ST1229	10.8	Universidad de la República, Uruguay	GCA_003584825.1
Streptomyces griseus	NBRC 13350	8.5*	(37)	GCA_000010605.1
Streptomyces hygroscopicus	XM201	12.0*	Shanghai Jiao Tong University	GCA_002021875.1
Streptomyces ipomoeae	78–51	10.7	This study	GCA_006547175.1
Streptomyces lividans	TK24	8.3*	(38)	GCA_000739105.1
S. ipomoeae	88–35	10.7	This study	GCA_006547185.1
S. ipomoeae	91–03	10.4	(28)	GCA_000317595.1
S. ipomoeae	B12321	10.9	This study	GCA_006547165.1
Streptomyces niveiscabiei	NRRL B-24457	9.5	(36)	GCA_001419795.1
Streptomyces puniciscabiei	DSM 41929	9.1	DOE Joint Genome Institute	GCA_006715785.1
S. puniciscabiei	NRRL B-24456	8.8	(36)	GCA_001419685.1
Streptomyces reticuliscabiei	NRRL B-24446	10.0	(36)	GCA_002154675.1
Streptomyces scabiei	87–22	10.1*	(39, 40)	GCA_000091305.1
S. scabiei	84–34	10.0	(14)	GCA_001550245.1
S. scabiei	85–08	10.0	(14)	GCA_001550215.1
S. scabiei	95–18	10.5	(14)	GCA_001550225.1
S. scabiei	96–06	9.0	(14)	GCA_001579685.1
S. scabiei	96–08	11.2	(14)	GCA_001550235.1
S. scabiei	96–15	9.2	(14)	GCA_001550295.1
S. scabiei	84–232	9.8	(14)	GCA_001572115.1
S. scabiei	S58	10.0	(31)	GCA_001485125.1
S. scabiei	NRRL B-2795	10.3	(36)	GCA_002156075.1
S. scabiei	NRRL B-2796	10.1	(36)	GCA_002155735.1
S. scabiei	NRRL B-2801	10.3	(36)	GCA_002155725.1
S. scabiei	NCPPB 4066	10.0	University of Exeter	GCA_000738715.1
S. scabiei	NCPPB 4086	10.5	University of Exeter	GCA_000738695.1
S. scabiei	NRRL B-16523	9.8	USDA/ARS/NCAUR	GCA_001005405.1
S. scabiei	NRRL B-24093	9.9	(36)	GCA_002155765.1
S. scabiei	ST129	9.8	Universidad de la República, Uruguay	GCA_003584815.1
Streptomyces stelliscabiei	NRRL B-24447	10.0	USDA/ARS/NCAUR	GCA_001008135.1
S. stelliscabiei	P3825	10.4	University of Exeter	GCA_001189035.1

(*Continued on next page*)

TABLE 1 Genome sequences used in this study (*Continued*)

Organism	Strain	Genome size (Mb)[a]	Reference or source	Genbank assembly accession no.
Streptomyces sp.	SirexAA-E	7.4	(41)	GCA_000177195.2
Streptomyces turgidiscabies	T45	10.6	(31)	GCA_001485145.1
S. turgidiscabies	Car8	10.8	(21, 28)	GCA_000331005.1
Streptomyces venezuelae	ATCC 10712	8.2	(42)	GCA_000253235.1
Streptomyces violaceusniger	Tu 4113	11.1*	US DOE Joint Genome Institute	GCA_000147815.3
Saccharopolyspora erythraea	NRRL 2338	8.2*	(43)	GCA_000062885.1

[a]Asterisk indicates genome sequence is complete.

used in this study are listed in Table 1 and a summary of the relevant characteristics of the four sequenced *S. ipomoeae* strains is presented in Table 2.

The draft sequence for *S. ipomoeae* 78-51 comprises 10,703,819 bp with 19-fold average coverage and was assembled into 348 contigs (N_{50} was 60 kb) with 8,734 predicted genes. The draft sequence for *S. ipomoeae* 88-35 comprises 10,654,678 bp with 17-fold average coverage. It contains 8,618 predicted genes and was assembled into 378 contigs (N_{50} was 58 kb). And the draft sequence for *S. ipomoeae* B12321 comprises 10,892,772 bp with 12-fold average coverage and it was assembled into 181 contigs (N_{50} was 135 kb) with 8,783 predicted genes. All three draft sequences have an average G + C content of 70%.

Two methods used for discriminating species based on genome sequence comparisons, namely average nucleotide identity (ANI) and *in silico* DNA-DNA hybridization (isDDH) were used here to assess the relatedness of strains 78-51, 88-35, 91-03, and B12321. In general, ANI values of 95%–96% correspond to the 70% DDH cutoff (44). Results from both methods supported the view that all four strains belong to the same species, despite B12321 being less related to the other strains (Fig. S1; Table S1). The findings here of lower relatedness of B12321 corroborate and extend previous experimental results (i.e., wet-lab DNA-DNA hybridizations, rep-PCR, and restriction enzyme fingerprinting) for the neotype strain (26, 45, 46).

Genome organization features for pathogenic and non-pathogenic *S. ipomoeae* strains

Draft genomes for each *S. ipomoeae* strain were built using the *S. scabiei* 87-22 genome as a reference and the sequences were then analyzed using the Artemis sequence viewer software (47). As noted earlier, the thaxtomin A gene cluster in scab pathogens is located within PAIs inserted at either the *bacA* gene (for *S. turgidiscabies*) or the *aviX1* gene (for *S. scabiei* and several other species). In contrast, the thaxtomin C gene cluster of *S. ipomoeae* strains 78-51, 88-35, and 91-03 is located at neither *bacA* nor *aviX1* with its relative position on the draft genomes for these strains as shown in Fig. 1. Moreover, as detailed later, thaxtomin genes in *S. ipomoeae* do not appear to be part of a genomic island. For the non-pathogenic strain B12321, the entire set of thaxtomin genes is missing from the genome, a finding that is consistent with previous studies that demonstrated a lack of thaxtomin C production for this strain (24, 25).

For the *bacA* locus, only the intact gene is present in all four *S. ipomoeae* strains with no duplication of its 3′ end or insertion of a genomic island. For *aviX1*, duplication of its 3′ end was evident for all three pathogenic *S. ipomoeae* strains, along with an

TABLE 2 Characteristics of sequenced *S. ipomoeae* strains[a]

Strain	State of origin	Pathogenicity	Inhibition group	Plasmid
78-51	LA	+	1	–
88-35	CA	+	2	–
91-03	NC	+	3	–
B12321	LA	–	NG[b]	+

[a]Characteristics as determined by Clark et al. (26).
[b]NG, not grouped.

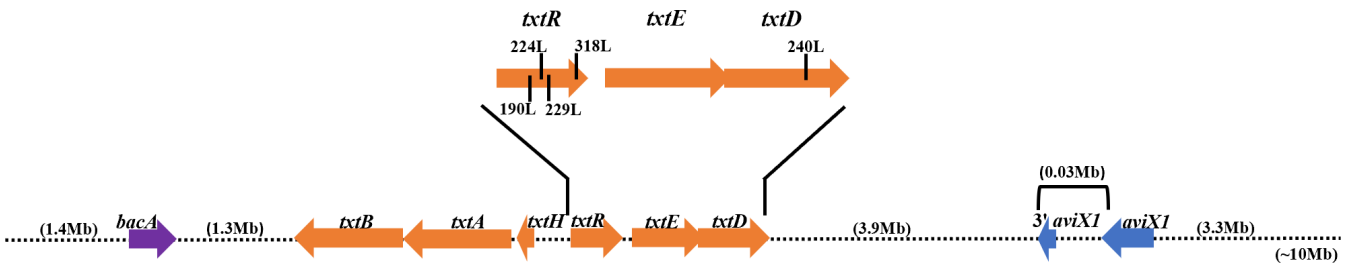

FIG 1 Schematic overview of the organization of the *S. ipomoeae* strains 78-51, 88-35, and 91-03 draft genomes showing the relative position of the thaxtomin C (*txt*) gene cluster in relation to the *bacA* and *aviX1* genes. The cluster is located 1.3 Mb downstream of *bacA* and 3.9 Mb downstream of *aviX1*, where a 30-kb island is inserted at the 3′ end of the gene. The upper enlarged portion of the figure highlights the positions of TTA leucine codons found in the *txt* cluster, with four located in *txtR* and one in *txtD*.

intervening sequence of approximately 30 kb (Fig. 1), whose size varied slightly among the three strains. In contrast, for strain B12321, we found only the intact *aviX1* gene with no duplication event or inserted sequence.

Closer inspection of the *aviX1* gene region of *S. ipomoeae* strains 78-51, 88-35, and 91-03 revealed features consistent with a potentially excisable genomic island, which we have named "aviX1Si." There are two copies of the sequence (5′ TTGAAGCGGAAC 3′), which immediately flank the island sequence, and which are designated *attL* and *attR* as shown in Fig. 2A. This same 12-bp sequence within *aviX1* is also the putative *att* site for TR in *S. scabiei* and other scab pathogens (14, 16, 18). Within aviX1Si toward *attL* is a gene (*intSi*), which is predicted to encode a site-specific tyrosine recombinase (integrase). Immediately upstream of *intSi* is an open reading frame (ORF) encoding a putative excisionase with a pI value of 9.22 (Fig. 2A). Alignment of the IntSi proteins of *S. ipomoeae* strains 78-51, 88-35, and 91-03 with similar proteins encoded by PAIs and ICEs from other *Streptomyces* spp. revealed that IntSi proteins share the three motif regions or "Boxes" that are characteristic of tyrosine recombinases (48). Included in Fig. 2B are the Box A (amino acids 199–221), Box B (amino acids 372–386), and Box C (amino acids 391–409) regions of the IntSi proteins with highlighting of the conserved arginine, arginine, and tyrosine residues that constitute the catalytic site of these proteins.

The presence of integrase and putative excisionase genes raised the possibility that aviX1Si is capable of excision from the *S. ipomoeae* chromosome. To test this notion, we screened genomic DNA isolated from broth cultures of each *S. ipomoeae* strain by PCR for an amplification product indicative of excision and circularization of aviX1Si. The relative positions of primers used in this assay are shown in Fig. 2A. For strains 78-51, 88-35, and 91-03, PCR involving primers 3 and 4 yielded an amplified product of 501 bp (Fig. 2C), which included the intact *att* site region of the excised circularized aviX1Si island. Additional PCR products of 460 bp (spanning *attL* of integrated aviX1Si) and 315 bp (spanning *attR*) were also seen for these three strains in reactions involving primers 1 and 2 and primers 4 and 5, respectively (Fig. 2C). DNA sequencing of all PCR products for strains 78-51, 88-35, and 91-03 confirmed their respective identities (data not shown). As expected, no *att*, *attL*, or *attR* amplicons were generated for strain B12321 (Fig. 2C). Taken together, the results indicate that within a population of *S. ipomoeae* cells containing integrated aviX1Si, spontaneous excision of the island does occur within a portion of those cells. Spontaneous excision in non-mating cells is known to occur for other *Streptomyces* integrative elements, including PAISt of *S. turgidiscabies* and TR of *S. scabiei* (18, 49).

Within aviX1Si of the three *S. ipomoeae* pathogenic strains are 25 predicted genes encoding various metabolic functions, transcriptional regulators, or hypothetical proteins (Table S2). Comparative analysis of the aviX1Si sequence using blastp (https://blast.ncbi.nlm.hih.gov/Blast.cgi) and phmmer (https://www.ebi.ac.uk/Tools/hmmer/search/phmmer) searches revealed that most of the genes (14 out of 25) match to other *Streptomyces* non-pathogens, while only four have matches with at least

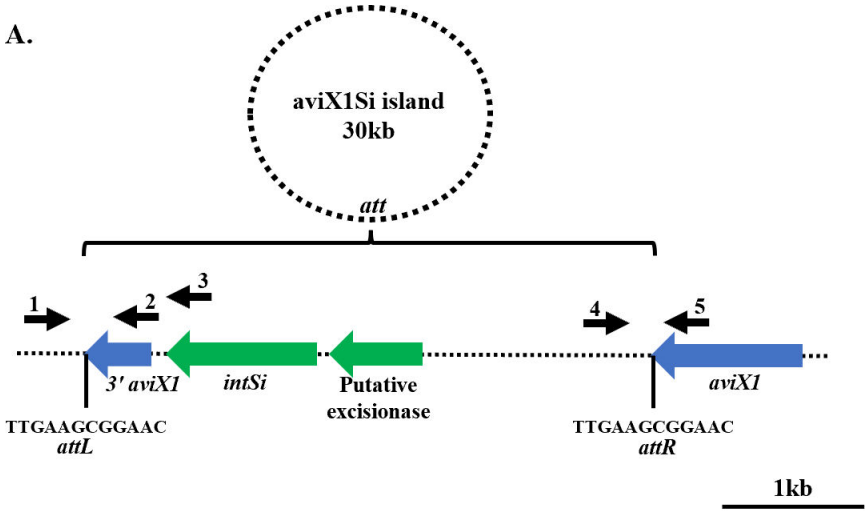

B.

S. turgidiscabies	YVWTFAMTGMRPAELYGLRPEYCHP
S. coelicolor	FFGCMYYAAARPAEVIGLRLQDCDL
S. acidiscabies	LVDFAHETGMRWGEIVGLRACYLDL
S. avermitilis	YIVVALLTGARTEELRALTWDHVFL
S. ipomoeae	TVYLQSGTGLRPSEALAFSSECRRT
S. scabiei	TIYLQAAAGLRISETLAFATECRRT
S. turgidiscabies	YLMRHGHKEWIDEDG
S. coelicolor	YDLRHAAVSTWLSSG
S. acidiscabies	HDYRHALASRLHARG
S. avermitilis	RELRHSFVSLLSDRG
S. ipomoeae	RSLRHFFASIALAHG
S. scabiei	HGLRHFFASTALANG
S. turgidiscabies	TESRMGHELA-GVEGLYSN
S. coelicolor	VAARAGHSV-AVLFRVYAK
S. acidiscabies	VQLMLGQERGGRVTWLYTH
S. avermitilis	ISRLVGHSGTAVTEEVYRK
S. ipomoeae	VSRWLGHRSVKATVDIYGH
S. scabiei	VSRWLGHKSIKTTVDIYGH

C.

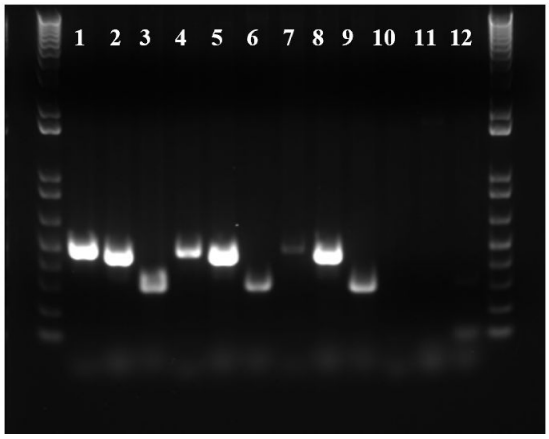

FIG 2 Sequence and excision details of the aviX1Si island. (A) Schematic overview of the aviX1Si island highlighting the attachment sites (*attL* and *attR* for the integrated island and *att* for the excised and circularized island) and the integrase (*intSi*) and putative excisionase genes. Numbered arrows represent

(Continued on next page)

FIG 2 (Continued)

the primers used to amplify sequences encompassing each attachment site as described in the text. (B) IntSi alignment with integrase proteins from other *Streptomyces* spp. showing the three conserved motif boxes. Conserved arginine, arginine, and tyrosine residues in red represent the catalytic site of the proteins. (C) A 1% agarose gel showing amplification of sequences encompassing the attachment sites in strains 78-51 (lanes 1–3), 88-35 (lanes 4–6), and 91-03 (lanes 7–9) but not B12321 (lanes 10–12); *attL* (460 bp; lanes 2, 5, and 8), *attR* (315 bp; lanes 3, 6, and 9), and *att* (501 bp; lanes 1, 4, and 7). The standard size markers in the 1-kb Plus DNA Ladder (New England Biolabs, Ipswich, MA, USA) are also shown.

one *Streptomyces* scab pathogen and seven do not match to any other *Streptomyces* species but rather have matches in other high-GC actinobacteria. Given the overall close phylogenomic relationship between *S. ipomoeae* and *S. scabiei* (28), we also performed a pairwise alignment between aviX1Si and the entire TR sequence of *S. scabiei* 87–22; however, apart from the integrase genes, there were no other sequence matches.

Notably missing from aviX1Si are genes predicted to be involved in conjugation (e.g., *traB* and *spd* functions of *Streptomyces* plasmid and ICE elements) (50, 51); thus, aviX1Si does not appear to fit the criteria of an ICE. However, its ability to excise from the host chromosome suggests that aviX1Si is a CIME (52), which may potentially be mobilizable from *S. ipomoeae* upon integration of an ICE in *cis* next to aviX1Si.

Using the ICEfinder algorithm (53), a search for ICEs within the *S. ipomoeae* draft genomes revealed that all three pathogenic strains contain at least one potential *traB*-containing ICE (also referred to as an actinomycete integrative and conjugative element or AICE) (Table S3); however, none of these AICEs are located near aviX1Si, with the closest being 0.7 Mb away in strain 78-51 (Table S3).

The presence of nearly identical versions of aviX1Si within the chromosomes of all three pathogenic *S. ipomoeae* strains raises the possibility that a function(s) encoded within the island is important for the virulence and/or persistence of this bacterium in its soil environment. To assess the conservation of aviX1Si further, we performed the same PCR screening on eight additional *S. ipomoeae* pathogenic strains recovered from various locations in the U.S. and Japan. Amplicons for *att*, *attL,* and *attR* were also generated for each of these eight additional pathogenic isolates (Fig. S2).

Distinguishing gene content of *S. ipomoeae*

An ortholog search was conducted by using OrthoFinder (54) in order to identify ortholog groups specific to pathogenic *S. ipomoeae* strains. Of the 53 genomes analyzed, 52 were *Streptomyces* spp. (single strains of 10 saprophytic species and 42 strains of plant-pathogenic species) plus an outgroup (*Saccharopolyspora erythraea*). The complete list of species and strains used, along with all orthogroups identified, is included in Table S4.

A total of 380 ortholog groups were found to be specific to one or more of the three pathogenic *S. ipomoeae* strains, and so these genes were neither present in strain B12321 nor in any of the saprophytic or other plant-pathogenic species analyzed (Fig. 3). We define these 380 ortholog groups as the *Streptomyces ipomoeae* pathogen-specific genome (SiPSG). Included within the SiPSG are 86 ortholog groups that are shared by all three pathogenic *S. ipomoeae* strains (Fig. 3), and we hypothesize that the latter group, in particular, may contain genes that contribute to the unique aspects of soil rot disease and/or promote persistence of *S. ipomoeae* in its natural soil environment.

Within these 86 shared groups, a handful appeared particularly noteworthy, including ortholog group OG0014661, which consists of genes encoding hemerythrin domain-containing proteins. Hemerythrin-like proteins constitute a large superfamily of proteins that have typically been studied for their ability to reversibly bind oxygen via their binuclear non-heme iron center (55). However, some members have been shown to have other biological roles, including NorA from *Ralstonia eutropha* and YtfE from *Escherichia coli*, which have the ability to bind nitric oxide (55). Given that thaxtomin production involves the production of nitric oxide (56), it is tempting to speculate that members of

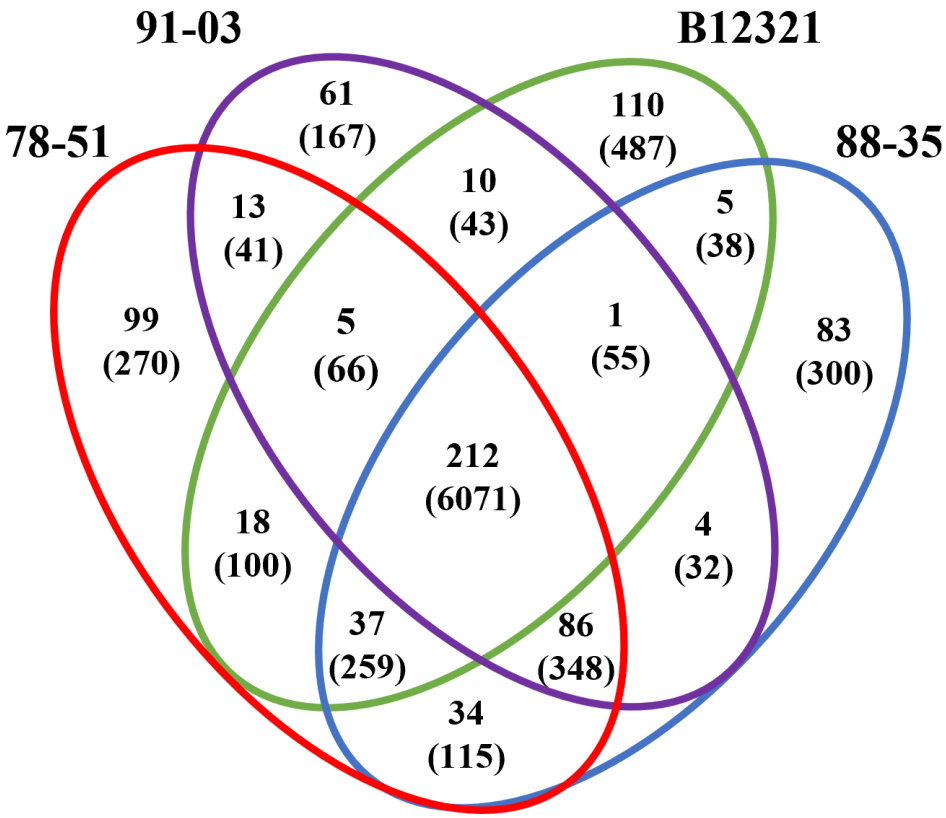

FIG 3 Distribution of ortholog genes in *S. ipomoeae*. The Venn diagram shows the distribution of ortholog gene groups specific to the four sequenced *S. ipomoeae* strains. The number of ortholog groups not specific to *S. ipomoeae* strains [i.e., present in the indicated *S. ipomoeae* strain(s) and in one or more of the other species used in the analysis] is shown in parentheses.

the OG0014661 ortholog group may play a role in regulating nitric oxide concentration in pathogenic *S. ipomoeae* strains.

Based on their annotation coupled with subsequent BLAST searches, both the OG0014676 and OG0014682 orthogroups comprise genes coding for CopA family copper-exporting P-type ATPases, while OG0014683 members encode CsoR copper-sensitive transcriptional regulators. Excess copper is highly toxic to living cells and copper defense is critical for virulence of many pathogenic bacteria (57). Copper is also known to be important for germination, development, and secondary metabolism in saprophytic *Streptomyces* spp. (58). Its potential role in the pathogenicity of *S. ipomoeae* remains to be evaluated and deserves experimental follow-up.

OG0014679 consists of members encoding PspA/IM30 family proteins. In *Streptomyces lividans*, PspA is present in both the cytoplasmic and the membrane fractions of substrate mycelia and is strongly induced under stress conditions that attack membrane integrity (59). In *Streptomyces coelicolor*, the gene coding for PspA was shown to be part of the σ^E regulon, which is involved in the cell envelope stress response (60). It is possible this protein could provide an advantage for *S. ipomoeae* pathogenic strains by protecting mycelia from extracytoplasmic stresses caused by defense compounds secreted by the host plant root system and/or molecules secreted by competing soil microbes.

Finally, group OG0014749 consists of the *txtH* orthologs for the three pathogenic *S. ipomoeae* strains, which were the only thaxtomin genes present in the SiPSG. MbtH-like family proteins such as TxtH are small polypeptides typically encoded in NRPS clusters, which appear to function as chaperones. A recent study provided evidence that the *S. scabiei* TxtH protein plays an important role in thaxtomin A biosynthesis by promoting proper folding of the TxtA and TxtB NRPSs (6). Moreover, MbtH-like proteins involved in

other biosynthetic pathways in *S. scabiei* could partially complement TxtH function in thaxtomin production and virulence on potato tuber tissue (6). Such complementation by heterologous MbtH-like proteins is common and has also been demonstrated in antibiotic and siderophore production pathways in saprophytic *Streptomyces* spp. (61, 62).

Previously, a *txtH* deletion mutant of *S. ipomoeae* strain 91-03 was still pathogenic on sweet potato adventitious roots (63), a result which was in contrast to those seen for other *txt* biosynthetic mutants of *S. ipomoeae* (25). A search here of the pathogenic *S. ipomoeae* genomes for *mbtH*-like genes besides *txtH* revealed several, including those found in gene clusters for metabolites cadaside A/B, scabichelin, and lipopeptide 8D1 (Table S5). Thus, it is possible that one or more of the MbtH-like proteins from these other pathways can complement *S. ipomoeae* TxtH for thaxtomin C production and pathogenicity on sweet potato.

In addition to defining the SiPSG, we also sought to evaluate the overall profile of known secondary metabolites (i.e., those previously characterized in other species) encoded here by the soil rot pathogen by using the genome mining algorithm antiSMASH (64). Besides a number of secondary metabolite gene clusters that were shared by *S. ipomoeae* and one or more of the scab pathogen species, there were two that were exclusive to *S. ipomoeae* in our analysis (Table S6).

One of these exclusive clusters was for phenolic lipid compounds known as alkylresorcinols (Fig. S3), which are synthesized via specialized type III polyketide synthases utilizing fatty acyl-CoA starter units and malonyl-CoA extender units (65, 66). In saprophytic *Streptomyces* spp., these phenolic lipids were shown to contribute to resistance to β-lactam antibiotics likely because they associate with the cytoplasmic membrane conferring rigidity to that structure (66). They are also common in plants where their involvement in plant defense as phytoanticipins and allelochemicals has been suggested due to their antimicrobial activity, which has been demonstrated *in vitro* (65).

A second cluster found only in *S. ipomoeae* strains in our analysis was for the biosynthesis of triacsins (Fig. S3), which were first discovered from a broth culture of *Streptomyces* sp. strain SK-1894 and are considered to be the most efficient acyl-CoA synthetase inhibitors (67). They are capable of blocking intracellular lipid accumulation through the action of a *N*-hydroxytriazene moiety in their structures, which is essential for inhibitory function (68). Long-chain fatty acyl-CoA plays important metabolic roles in lipid biosynthesis and β-oxidation of fatty acids and regulates these processes (e.g., by allosteric inhibition) as well as other cellular pathways. The conversion of free long-chain fatty acids to acyl-CoA is catalyzed by acyl-CoA synthetase, making it a pivotal enzyme in the pathway (68).

Finally, with regard to the interstrain inhibition phenotype of *S. ipomoeae*, the group III inhibitor ipomicin was previously identified as a bacteriocin, which consists of a 10 kDa cationic protein with bacteriolytic activity. Its structural gene *ipoA* was cloned and sequenced from a cosmid library of the group III strain 91-03 (27). Interestingly, a search here for the *ipoA* gene in the genome sequences of strains 78-51 (group I) and 88-35 (group II) revealed that they both contained the intact *ipoA* gene with no mutations relative to the copy found in strain 91-03 (Fig. S4). A copy of *ipoA* containing four silent mutations was also found in the genome of strain B12321 (Fig. S4), which displayed variable interstrain reactions such that it could not be placed into an inhibition group (26). Further study is needed to determine whether the protein product of *ipoA* is produced by non-group III strains and, if so, what its relation is to the active ipomicin inhibitor produced by group III strains. Since many bacteriocins undergo post-translational modifications to become active (69), it is possible that ipomicin is similarly modified in group III strains to become an active inhibitor, whereas in non-group III strains, it is either not produced in an active form or simply not produced at all.

Further characterization of the *txt* locus of *S. ipomoeae*

Given that thaxtomin genes are typically part of mobile pathogenicity islands in *Streptomyces* scab pathogens, we assessed the potential for the *txt* locus of *S. ipomoeae* to be associated with a genomic island. Using Artemis, we manually examined the sequences encompassing the thaxtomin genes for evidence of a genomic island (e.g., duplicated sequences, integrase genes, conjugation genes, etc.) but found none by this method. Two genomic island prediction programs, IslandViewer (70) and Alien Hunter (71), also did not predict an island in this genomic region (data not shown).

We also assayed for conjugative transfer of the thaxtomin genes (i.e., as part of an undetected mobile island) to a recipient. The potential *S. ipomoeae* donor was a derivative of strain 91-03 in which the apramycin-resistant, colE1-based shuttle plasmid pSIP62 was integrated by homologous recombination at the *txt* locus (see Materials and Methods for details), while the potential recipient was *Streptomyces diastatochromogenes*, a saprophytic species that has previously been shown to acquire a pathogenic phenotype upon receipt of PAIs from *Streptomyces* scab pathogen species (13–16). Under conditions in which transfer of TR from *S. scabiei* to *S. diastatochromogenes* was readily observed, no transconjugants were detected following three independent mating attempts involving *S. ipomoeae* strain 91-03(pSIP62) and *S. diastatochromogenes* (Table 3). Thus, the *in silico* and experimental approaches undertaken here provided no evidence that the thaxtomin gene cluster is part of a genomic island in *S. ipomoeae*.

It is possible that at one time the thaxtomin A gene cluster of *S. scabiei* was not part of a genomic island, but that a recombination event resulted in its repositioning at *aviX1* into what has become the TR. In recent decades, horizontal transmission of the TR has likely fueled the emergence of additional scab pathogen species (28). In contrast, *S. ipomoeae* remains the only species known to harbor the thaxtomin C cluster and cause soil rot disease (1).

In the previous phylogenomic study involving *S. scabiei* 87-22 and *S. ipomoeae* 91-03, the results indicated a close overall relationship between the two species in terms of their core genomes and gene content, but their *txt* gene clusters appeared to be less related and so may have diverged (28). To evaluate the relationship among the thaxtomin genes of the soil rot and scab pathogens more comprehensively, the *txt* genes of 31 strains from six thaxtomin-positive scab pathogen species, along with those of the three pathogenic *S. ipomoeae* strains, were used to build individual phylogenetic trees for each *txt* gene, and the trees were then summarized into one consensus tree (Fig. 4). The position of the thaxtomin genes for the three *S. ipomoeae* strains in a separate well-supported clade in the consensus tree highlights the strong divergence of these genes from their counterparts in all the scab pathogen species examined.

The *S. scabiei txtR* gene contains a single TTA codon (9), and a *bldA* mutant of *S. scabiei* was found to be defective for thaxtomin A production and virulence (12). Interestingly, upon inspection of the thaxtomin C gene clusters of *S. ipomoeae* strains 91-03, 88-35, and 78–51, we found their *txtR* genes all contained four TTA codons at the positions indicated in Fig. 1. An additional TTA codon was found within the *txtD* biosynthetic gene for all three pathogenic strains (Fig. 1). Subsequent sequence analysis of the *txtR* genes from seven additional pathogenic *S. ipomoeae* strains isolated from diverse geographic locations confirmed the presence of the same four TTA codons in *txtR* in all strains examined (Fig. S5).

TABLE 3 Conjugation assay to test transfer of the thaxtomin C gene cluster from *S. ipomoeae* to *S. diastatochromogenes*[a]

Donor	Recipient (*S. diastatochromogenes*)	Transconjugants
2.8×10^5 *S. scabiei* 87-22 Δ*txtH*	$>1.2 \times 10^{10}$	2.8×10^5
3.2×10^6 *S. ipomoeae* 91-03(pSIP62)	$>1.2 \times 10^{10}$	0

[a]Following three independent conjugation assays per mating pair, colony-forming units for donors (apramycin-resistant), recipients (streptomycin-resistant), and transconjugants (apramycin- and streptomycin-resistant) were quantified on relevant selective media and the averages are presented.

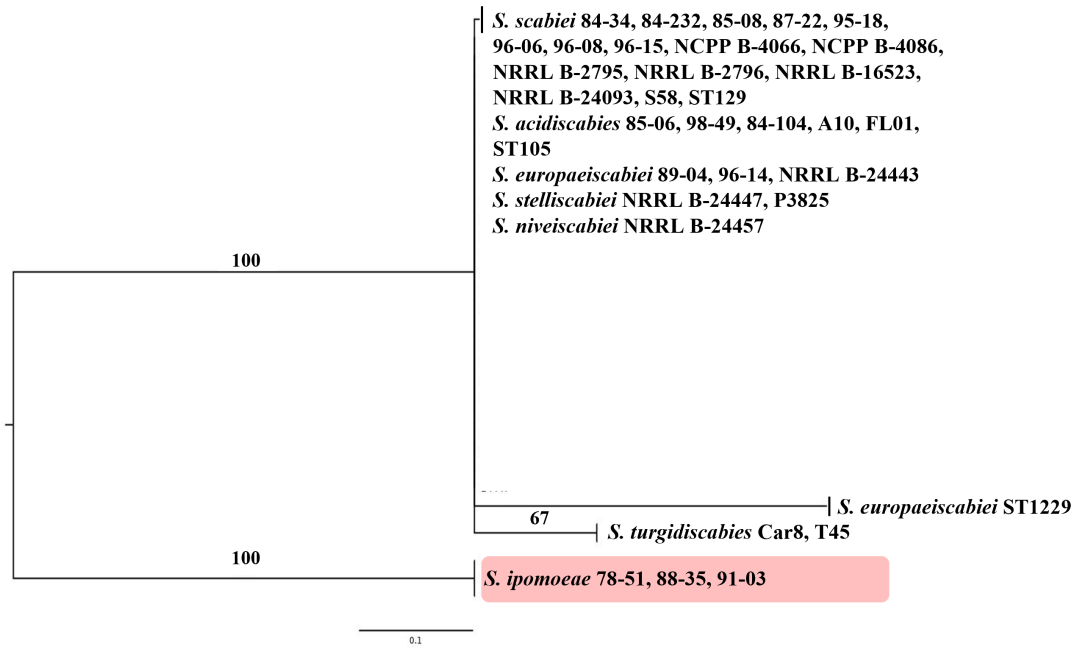

FIG 4 Thaxtomin cluster consensus tree summarized from individual phylogenetic trees for each *txt* gene by using SumTrees from the DendroPy package. The *txt* genes (except for *txtC*) of 31 strains from six thaxtomin-positive scab pathogen species, in addition to those of the three pathogenic *S. ipomoeae* strains, were used. The position of the three pathogenic *S. ipomoeae* strains in the consensus tree is highlighted. Bootstrap support (based on 1,000 resamplings of the data set) is presented at each node and represents percentages.

The presence of five TTA codons in the *txt* gene cluster of *S. ipomoeae* raises the possibility of exceptional *bldA* control of thaxtomin production and virulence, especially if the *txtR* gene, where the majority of TTA codons reside, plays a pivotal role in the pathogenicity of this bacterium. To address this notion further, we constructed an in-frame *txtR* deletion mutant of strain 91-03 (i.e., strain DG12; see Materials and Methods for details), and then tested DG12 for virulence in a sweet potato adventitious root assay. Root necrosis was evaluated by using the scale described previously (72). As shown in Fig. 5 and Table 4, exposure of roots to strain DG12 resulted in no necrosis, which was similar to uninoculated control roots or those exposed to DG12 carrying the empty plasmid vector pSET152. Meanwhile, the complemented mutant DG16 appeared to be restored to full virulence based on its necrosis in comparison to the parent (Fig. 5 and Table 4).

To assess thaxtomin C production by strains DG12 and DG16, sweet potato storage roots were infected with individual *S. ipomoeae* strains, and extracts were prepared as described previously (25) and then analyzed here by liquid chromatography-mass spectrometry (LC-MS). Extracts of storage roots infected with the parental strain 91-03 or

TABLE 4 Adventitious root assay necrosis ratings[a]

	Vine cutting				
Strain[b]	1	2	3	4	Ave.[c]
VGM only	0	0	0[d]	0	0.00
91-03	2	4[d]	5	5	4.00
DG12	0	0	0[d]	0	0.00
DG12(pSET152)	0	0[d]	1	0	0.25
DG16	5	5	5[d]	5	5.00

[a]Necrosis ratings for four independent Jewel cultivar vine cuttings inoculated with the indicated *S. ipomoeae* strains using a 0–5 scale in which 0 = no necrosis and 5 = 100% necrosis.
[b] *S. ipomoeae* strains; VGM, vermiculite growth medium.
[c]Average rating per *S. ipomoeae* strain treatment.
[d]Plant roots shown in Fig. 5.

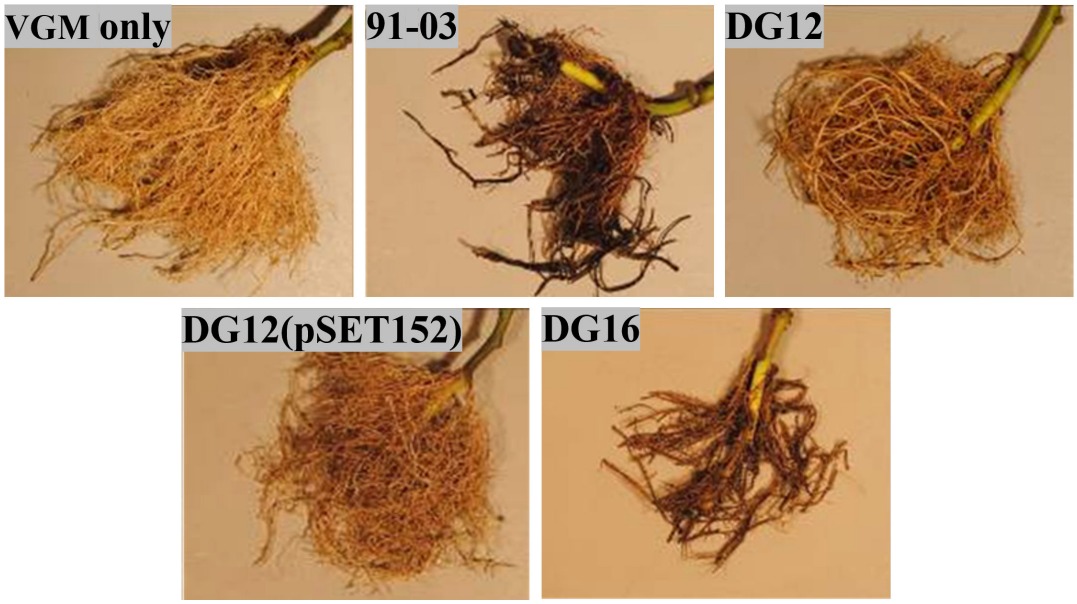

FIG 5 Sweet potato adventitious root pathogenicity assay. Cultivar Jewel plants grown in soil amended with sterile vermiculite growth medium (VGM) or with VGM cultures of the individual *S. ipomoeae* strains are indicated. Four replicate plants were used per strain, and the roots were scored for necrosis following completion of the assay.

the thaxtomin biosynthetic mutant DG5 (25) served as positive and negative controls for thaxtomin production, respectively.

As shown in Fig. 6, sweet potato extracts infected with strain 91-03 yielded the [M + Na]$^+$ ion of thaxtomin C at *m/z* 415.1403 (positive ion mode), while as expected, this ion was missing for DG5-infected tissue. For the *txtR* mutant DG12, only a trace amount of the [M + Na]$^+$ thaxtomin C ion was evident, while this ion was readily seen for the complemented mutant DG16. Additional thaxtomin C adducts [i.e., the [M + H]$^+$ ion at

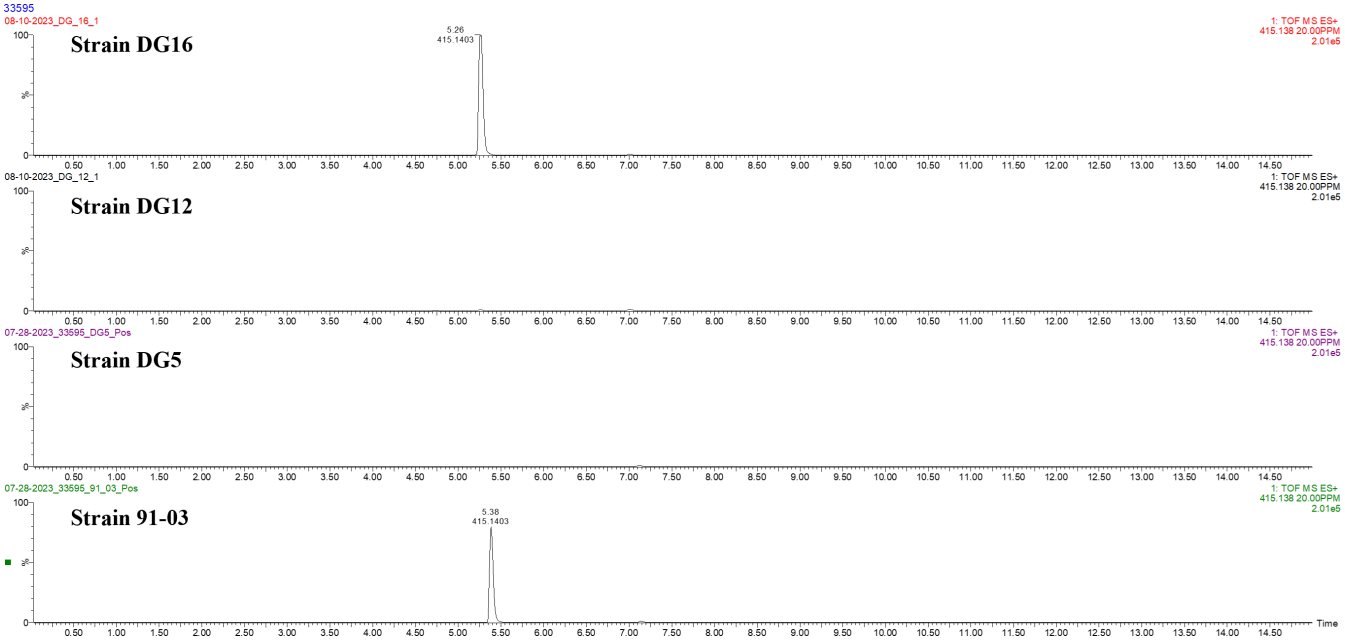

FIG 6 Extracted ion chromatograms for the [M + Na]$^+$ ion of thaxtomin C. Extracts of Beauregard sweet potato storage roots that had been infected with individual *S. ipomoeae* strains were prepared and subjected to LC-MS, which consisted of separation of compounds on a Waters Acquity Premiere BEH C18 column followed by further analysis on a Waters Synapt XS Mass Spectrometer.

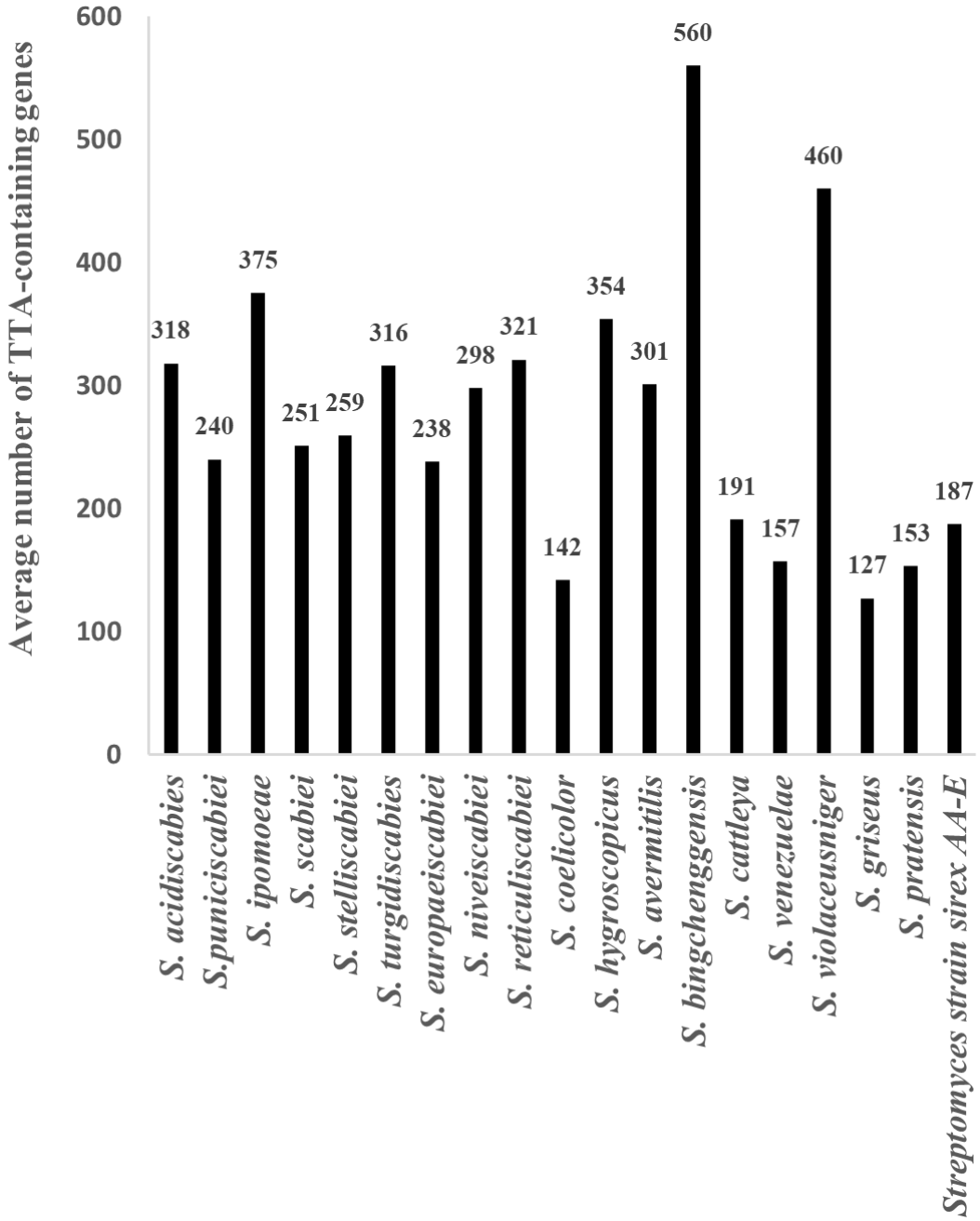

FIG 7 Average number of TTA-containing genes in plant-pathogenic and saprophytic *Streptomyces* spp. as determined by performing genome-wide in-frame searches for TTA codons using the perl script described by Chandra and Chater (11).

m/z 393.1531 and the $[2M + Na]^+$ ion at *m/z* 807.2886 (both in positive ion mode)] were also detected in relatively smaller amounts in our analysis (data not shown). Area under the curve values for each ion assigned to thaxtomin C were determined and summed for each strain (Table S7); the presence of multiple thaxtomin C ions reinforces the notion that the *txtR* mutant DG12 produces trace quantities of thaxtomin C on the sweet potato host. Thus, our LC-MS analysis, in combination with the adventitious root assay results (Fig. 5), provides strong evidence that the TxtR protein of *S. ipomoeae* is critical for the induction of thaxtomin C production and pathogenicity in this species.

Comparative TTA codon usage for *S. ipomoeae* relative to other *Streptomyces* species

The TTA content of the thaxtomin C cluster raised the possibility that *S. ipomoeae* may have evolved greater TTA codon usage in general, and therefore *bldA* control, as compared to *S. scabiei* and potentially other *Streptomyces* spp. To explore this notion further, we performed genome-wide in-frame searches for TTA codons using a previously described perl script (11).

Genome-wide usage was compared for strains of *S. ipomoeae*, *Streptomyces* scab pathogen species, and several saprophytic species. The average number of TTA-containing genes for the four *S. ipomoeae* strains (375) was the highest seen among the nine plant-pathogenic species examined and represented a 50% increase over the average for *S. scabiei* (Fig. 7). However, the vast majority of TTA-containing genes in *S. ipomoeae* still contain only one (~91%) or two (~7%) TTA codons (Fig. S6), which is consistent with TTA codon usage in other *Streptomyces* spp. (73). Thus, the presence of four TTAs in *txtR* and five within the thaxtomin C cluster appears to be exceptional for *S. ipomoeae*. Finally, a search for homologous *bldA* gene sequences within the four *S. ipomoeae* strains confirmed that each contained a single *bldA* gene, which is identical or very closely related to the *bldA* gene of *S. scabiei* (Fig. S7). Overall, our results here set the stage for future research aimed at elucidating the impact of *bldA* regulation on thaxtomin C production and virulence in the soil rot pathogen.

MATERIALS AND METHODS

S. ipomoeae strains

All *S. ipomoeae* pathogenic isolates and the non-pathogenic neotype strain B12321 used in this study were described previously (26). The thaxtomin biosynthetic mutant DG5 is a previously described Δ*txtA* derivative of strain 91-03 (25).

Genome sequencing

The genomes of *S. ipomoeae* strains 78-51, 88-35, and B12321 were sequenced (at the J. Craig Venter Institute) by using a combination of Sanger sequencing and Roche 454 pyrosequencing technologies. Sequencing of both medium-insert (10–12 kb) and small-insert (4–5 kb) plasmid libraries generated sequence reads, which were then assembled using Celera Assembler v. 4.1 (74). GLIMMER v. 3.02 was used to predict coding sequences (75). Automatic annotation of genomes was performed using the software Prokka (76) together with a brief manual annotation to check the integrity of the annotated sequences. Draft genomes were constructed using ABACAS (77) with *S. scabiei* strain 87-22 as the reference genome and they were then visualized and manipulated further using Artemis (47). Sequences were deposited as whole-genome shotgun sequencing projects in the GenBank database with the following accession numbers: *S. ipomoeae* 78-51 (NZ_SPAY00000000), 88-35 (NZ_SPAZ00000000), and B12321 (NZ_SPBA00000000). *S. ipomoeae* strains are available upon request.

Gene content analysis and phylogenetic tree construction

Ortholog analysis was performed using OrthoFinder v2.3.3 with genome sequences downloaded directly from GenBank. OrthoFinder uses protein fasta files as input and runs a core algorithm described previously (54, 78). The program uses the MCL clustering algorithm to organize genes into orthogroups and STAG + STRIDE for tree inference. The *txt* consensus tree was constructed by first building individual trees for each *txt* gene (except *txtC*) from every *Streptomyces* plant pathogenic strain where the cluster was found and then summarizing all trees in a majority-rule consensus using the SumTrees program from the DendroPy package. For tree visualization, the software used was FigTree v1.4.3 (http://tree.bio.ed.ac.uk/software/figtree/). The Venn diagram

was constructed using the Venn diagram R package from the CRAN repository (https://cran.r-project.org/) following the manual instructions for quadruple Venn diagrams. For in-frame TTA codon searches in *Streptomyces* genomes, the Perl script developed by Chandra and Chater (11) was used (available at GitHub, https://github.com/streptomyces/inframeTTA). Secondary metabolite cluster searches were performed by using the antiSMASH website (https://antismash.secondarymetabolites.org/) as described (64). For genomic island predictions, two programs, IslandViewer (70) and AlienHunter (71), were used without modifications to the methods. Detection of AICEs was performed by using the ICEfinder website (https://bioinfo-mml.sjtu.edu.cn/ICEfinder/ICEfinder.html) (53).

PCR analysis of the aviX1Si island

Genomic DNA isolation from tryptic soy broth cultures of *S. ipomoeae* strains was performed by using a ZymoBIOMICS DNA Miniprep Kit (Zymo Research, Irvine, CA, USA) according to the manufacturer's instructions. Primers were synthesized by MilliporeSigma (Burlington, MA, USA) and were designed to amplify fragments indicative of attachment sites associated with the aviX1Si island using the PrimerQuest and OligoAnalyzer Tool from the Integrated DNA Technologies website (https://www.idtdna.com/pages). As depicted in Fig. 2, a 460-bp fragment encompassing *attL* was generated using primers 1 and 2 (i.e., 5′ GTCCTGCAGAACGCCAT 3′ and 5′ CCTTCTTGATCAGCGGA AAGA 3′), while a 315-bp fragment including *attR* was generated using primers 4 and 5 (5′ AGCACGGGAAACAGCAAAGG 3′ and 5′ CGCCTGGACCATCAAGAA 3′). Meanwhile, a 501-bp fragment encompassing the *att* site of the excised circularized aviX1Si island was generated using primers 3 and 4 (5′ GGACGGCAAGGCAAAGTA 3′ and 5′ AGCACGGGAAA CAGCAAAGG 3′).

Cloning and sequencing of *txtR* genes from additional *S. ipomoeae* strains

Genomic DNA from *S. ipomoeae* strains was isolated by using the method described in the previous section. Primers 5′-CAGCGCAAAGAAGCATCCAG-3′ and 5′-CGAGTGGCCGAT ACCTCTTC-3′ (MilliporeSigma, Burlington, MA, USA) were designed using the finished *S. ipomoeae* 91-03 thaxtomin gene cluster sequence (25) and they were used to amplify a 1,254-bp sequence that included the entire *txtR* gene. Individual amplicons were ligated into linearized pMiniT 2.0 vector and transformants were obtained by using NEB 10-beta competent *Escherichia coli* cells all as contained in a NEB PCR cloning kit (New England Biolabs, Ipswich, MD, USA) and according to the manufacturer's instructions. Isolation of plasmid DNA from ampicillin-resistant transformants was performed by using a QIAprep Spin Miniprep Kit (Qiagen, Germantown, MD, USA). Recombinant plasmids were verified by relevant restriction enzyme digestions, and sequencing of cloned amplicon sequences was performed by Eurofins Genomics (Louisville, KY, USA) by using Sp6 and T7 universal primers. Clone Manager, version 2.0 (Sci Ed Software, Westminster, CO, USA) was used to align all *txtR* ORF sequences relative to the *txtR* sequence of strain 91–03 (25).

Construction of an in-frame txtR deletion mutant and complementation analysis

Relative to *txtR*, a 2.0-kb upstream fragment and a 1.6-kb downstream fragment were amplified by PCR from pSIP45 (25) with primers txtR5XbaI5, 5′-CGCATCTAGAGTGTAT CTCGCCTGT and txtR5KpnI3, 5′-TCAAGGTACCATACAAAGCGCAAGC, and with primers txtR3KpnI5, 5′-ACTAGGTACCCCAATTCTGGAACCG and txtR3EcoRI3, 5′-AGGAGAATTCGAG GTTGTCGTTCCA, respectively. The upstream fragment was digested with *Xba*I and *Kpn*I and cloned into the *E. coli* vector pSP72 (Promega, Madison, WI, USA) at the same restriction sites to generate pSP72-txtR5′. The downstream fragment was then digested with *Kpn*I and *EcoR*I and cloned into the same sites of pSP72-txtR5′ to create pSP72-txtR5′-txtR3′, which thus has an in-frame deletion within *txtR*. The 3.6-kb insert was removed by digesting with *Xba*I and *EcoR*I and ligated into the apramycin-resistant (Am^r)

plasmid pOJ260 (79) at the same sites, resulting in pSIP62, which was then used to transform *E. coli* strain S17.1 (79).

Intergeneric conjugation of pSIP62 to *S. ipomoeae* strain 91-03, selection of Am^r single-crossover transconjugants, and screening for Am-sensitive (Am^s) double recombinants were carried out as described previously (25). After screening more than 3,300 colonies, four Am^s colonies were identified of which three appeared to have the *txtR* deletion as determined by relevant PCR. Mutants were then verified by Southern blotting, which involved *BamH*I-digested or *BsiW*I-digested DNA of each clone, and a 481-bp radiolabeled probe fragment, which was produced via a PCR-based random priming reaction (25) with txtH5KpnI5, 5′-ATAAGGTACCAAGCAACTCCGAGGG, and txtR5KpnI3 as primers and pSIP45 as template. All other Southern blotting details were as described previously (25). By this procedure, mutant isolates displayed a hybridized *Bam*HI fragment of 1.9 kb (compared to a band of 2.8 kb for strain 91-03) and a hybridized *Bsi*WI fragment of 1.2 kb (compared to a 2.1-kb fragment for 91-03) (data not shown). One of the mutant isolates was chosen for further study and designated strain DG12.

To complement DG12, a 1.3-kb fragment containing the entire *txtR* gene was amplified by PCR from pSIP45 using primers txtR5XbaI, 5′-ACCCTCTAGACAGCTTTGCAT TTCA and txtR3EcoRI, 5′- CCAGGAATTCGTACTACGGTAAGGA, and the resulting fragment was digested with *Xba*I and *EcoR*I and cloned into these sites on pSP72 to create plasmid pSIP64. The pSIP64 insert was then released by digesting with *Xba*I and *EcoR*I, cloned into the same sites of pSET152 (79), and the resulting construct (pSIP65) was conjugated from *E. coli* S17.1 to *S. ipomoeae* DG12. Transconjugants were selected by overlaying with Am and nalidixic acid and verified by PCR as described (80). One transconjugant was designated *S. ipomoeae* DG16 and used for further study.

Pathogenicity assay

Pathogenicity assays involving sweet potato cultivar Jewel were conducted as described in reference (25). Necrosis on adventitious roots was rated per the scale previously described (72).

LC-MS analysis of thaxtomin C

Sweet potato storage roots of the Beauregard variety were infected with individual *S. ipomoeae* strains and extracts of the infected tissue were prepared as previously described (25). Dried extracts were resuspended in methanol at 50 µg/mL, and 1 µL aliquots were injected into the LC-MS system, which comprises a Waters Acquity Premiere UPLC and Waters Synapt XS mass spectrometer. Samples were separated on a Waters Acquity Premiere BEH C18 column (2.1 mm ID, 100 mm length, 1.7 µm pores) using a flow rate of 400 µL/min. The LC run was performed using a gradient program and employing two mobile phases: A, water with 0.1% formic acid and B, acetonitrile. Following a 2-min isocratic hold, mobile phase B was increased from 5% to 95% over the course of 6 min. A reference mass was sprayed every 15 s to recalibrate the spectra. The capillary voltage was kept at 0.8 kV in positive mode and 1.5 kV in negative mode, and data were acquired in the MS^E mode at an acquisition rate of 5 Hz. Data analysis was performed by using Waters MassLynx software (version 4.2).

Mating assay

Conjugations were performed and quantified on International *Streptomyces* Project Medium 4 and as otherwise described previously (81). The *S. ipomoeae* 91-03 derivative used for conjugations contains plasmid pSIP62, which, as described above, was integrated by homologous recombination at the *txt* locus. The *S. scabiei* 87-22 Δ*txtH* donor strain contains the apramycin-resistance gene in the place of *txtH* (14). The potential recipient for all conjugation assays was *S. diastatochromogenes* strain ATCC 12309, which is naturally streptomycin-resistant (13).

ACKNOWLEDGMENTS

Mass spectrometry experiments were performed at the LSU Mass Spectrometry Facility (MSF). We gratefully acknowledge Govind Chandra for helpful discussions and assistance with TTA codon searches using perl scripts. We also thank Imana Power for providing sweet potato storage roots and other supplies.

This work was funded in part by a fellowship to N.R.S. from the Coordinating Agency for Advanced Training of Graduate Personnel (CAPES) via the Science without Borders Program within the Ministry of Education of Brazil.

This work was also supported by the National Research Initiative of the U.S. Department of Agriculture (USDA) Cooperative State Research, Education, and Extension Service under grant number 2007-35600-17813 and the USDA National Institute of Food and Agriculture (NIFA) under Hatch project numbers LAB94112, LAB94337, and LAB94531.

AUTHOR AFFILIATIONS

[1]Department of Biological Sciences, Louisiana State University, Baton Rouge, Louisiana, USA
[2]Department of Plant Pathology, University of Florida, Gainesville, Florida, USA
[3]Department of Plant Pathology and Crop Physiology, Louisiana State University Agricultural Center, Baton Rouge, Louisiana, USA
[4]Department of Chemistry, Louisiana State University, Baton Rouge, Louisiana, USA
[5]Laboratory of Integrative Cancer Immunology, Center for Cancer Research, National Cancer Institute, National Institutes of Health, Bethesda, Maryland, USA

AUTHOR ORCIDs

Gregg S. Pettis http://orcid.org/0000-0002-5468-8870

FUNDING

Funder	Grant(s)	Author(s)
U.S. Department of Agriculture (USDA)	2007-35600-17813	Gregg S. Pettis
U.S. Department of Agriculture (USDA)	LAB94112	Christopher A. Clark Gregg S. Pettis
U.S. Department of Agriculture (USDA)	LAB94337	Christopher A. Clark Gregg S. Pettis
U.S. Department of Agriculture (USDA)	LAB94531	Christopher A. Clark Gregg S. Pettis

AUTHOR CONTRIBUTIONS

Natasha R. Soares, Investigation, Writing – original draft | José C. Huguet-Tapia, Investigation | Dongli Guan, Investigation | Christopher A. Clark, Formal analysis, Funding acquisition, Methodology | Kuei-Ting Yang, Investigation | Olivia R. Kluchka, Investigation | Raju S. Thombal, Methodology | Rendy Kartika, Methodology, Supervision | Jonathan H. Badger, Formal analysis, Methodology | Gregg S. Pettis, Conceptualization, Funding acquisition, Supervision, Writing – review and editing

ADDITIONAL FILES

The following material is available online.

Supplemental Material

Fig. S1-S7 and Tables S1-S3, S5 and S7 (AEM00308-23-s0001.pdf). All supplemental info except Tables S4 and S6.
Table S4 (AEM00308-23-s0002.xlsx). Ortholog gene search results.
Table S6 (AEM00308-23-s0003.xlsx). antiSMASH secondary metabolite cluster analysis.

REFERENCES

1. Li Y, Liu J, Díaz-Cruz G, Cheng Z, Bignell DRD. 2019. Virulence mechanisms of plant-pathogenic *Streptomyces* species: An updated review. Microbiology (Reading) 165:1025–1040. https://doi.org/10.1099/mic.0.000818
2. Loria R, Kers J, Joshi M. 2006. Evolution of plant pathogenicity in *Streptomyces*. Annu Rev Phytopathol 44:469–487. https://doi.org/10.1146/annurev.phyto.44.032905.091147
3. Barry SM, Kers JA, Johnson EG, Song L, Aston PR, Patel B, Krasnoff SB, Crane BR, Gibson DM, Loria R, Challis GL. 2012. Cytochrome P450-catalyzed L-tryptophan nitration in thaxtomin phytotoxin biosynthesis. Nat Chem Biol 8:814–816. https://doi.org/10.1038/nchembio.1048
4. Healy FG, Wach M, Krasnoff SB, Gibson DM, Loria R. 2000. The txtAB genes of the plant pathogen *Streptomyces acidiscabies* encode a peptide synthetase required for phytotoxin thaxtomin A production and pathogenicity. Mol Microbiol 38:794–804. https://doi.org/10.1046/j.1365-2958.2000.02170.x
5. Johnson EG, Krasnoff SB, Bignell DRD, Chung W-C, Tao T, Parry RJ, Loria R, Gibson DM. 2009. 4-Nitrotryptophan is a substrate for the non-ribosomal peptide synthetase TxtB in the thaxtomin A biosynthetic pathway. Mol Microbiol 73:409–418. https://doi.org/10.1111/j.1365-2958.2009.06780.x
6. Li Y, Liu J, Adekunle D, Bown L, Tahlan K, Bignell DRD. 2019. TxtH is a key component of the thaxtomin biosynthetic machinery in the potato common scab pathogen *Streptomyces scabies*. Mol Plant Pathol 20:1379–1393. https://doi.org/10.1111/mpp.12843
7. Healy FG, Krasnoff SB, Wach M, Gibson DM, Loria R. 2002. Involvement of a cytochrome P450 monooxygenase in thaxtomin A biosynthesis by *Streptomyces acidiscabies*. J Bacteriol 184:2019–2029. https://doi.org/10.1128/JB.184.7.2019-2029.2002
8. Kers JA, Wach MJ, Krasnoff SB, Widom J, Cameron KD, Bukhalid RA, Gibson DM, Crane BR, Loria R. 2004. Nitration of a peptide phytotoxin by bacterial nitric oxide synthase. Nature 429:79–82. https://doi.org/10.1038/nature02504
9. Joshi MV, Bignell DRD, Johnson EG, Sparks JP, Gibson DM, Loria R. 2007. The Arac/XylS regulator TxtR modulates thaxtomin biosynthesis and virulence in *Streptomyces scabies*. Mol Microbiol 66:633–642. https://doi.org/10.1111/j.1365-2958.2007.05942.x
10. Chater KF, Chandra G. 2008. The use of the rare UUA Codon to define "expression space" for genes involved in secondary metabolism, development and environmental adaptation in *Streptomyces*. J Microbiol 46:1–11. https://doi.org/10.1007/s12275-007-0233-1
11. Chandra G, Chater KF. 2008. Evolutionary flux of potentially *bldA*-dependent *Streptomyces* genes containing the rare leucine codon TTA. Antonie Van Leeuwenhoek 94:111–126. https://doi.org/10.1007/s10482-008-9231-5
12. Bignell DRD, Francis IM, Fyans JK, Loria R. 2014. Thaxtomin A production and virulence are controlled by several *bld* gene global regulators in *Streptomyces scabies*. Mol Plant Microbe Interact 27:875–885. https://doi.org/10.1094/MPMI-02-14-0037-R
13. Kers JA, Cameron KD, Joshi MV, Bukhalid RA, Morello JE, Wach MJ, Gibson DM, Loria R. 2005. A large, mobile pathogenicity island confers plant pathogenicity on *Streptomyces* species. Mol Microbiol 55:1025–1033. https://doi.org/10.1111/j.1365-2958.2004.04461.x
14. Zhang Y, Bignell DRD, Zuo R, Fan Q, Huguet-Tapia JC, Ding Y, Loria R. 2016. Promiscuous pathogenicity islands and phylogeny of pathogenic *Streptomyces* spp. Mol Plant Microbe Interact 29:640–650. https://doi.org/10.1094/MPMI-04-16-0068-R
15. Zhang Y, Jiang G, Ding Y, Loria R. 2018. Genetic background affects pathogenicity Island function and pathogen emergence in *Streptomyces*. Mol Plant Pathol 19:1733–1741. https://doi.org/10.1111/mpp.12656
16. Zhang Y, Loria R. 2017. Emergence of novel pathogenic *Streptomyces* species by site-specific accretion and cis-mobilization of pathogenicity islands . Mol Plant Microbe Interact 30:72–82. https://doi.org/10.1094/MPMI-09-16-0190-R
17. Lerat S, Simao-Beaunoir AM, Beaulieu C. 2009. Genetic and physiological determinants of *Streptomyces scabies* pathogenicity. Mol Plant Pathol 10:579–585. https://doi.org/10.1111/j.1364-3703.2009.00561.x
18. Chapleau M, Guertin JF, Farrokhi A, Lerat S, Burrus V, Beaulieu C. 2016. Identification of genetic and environmental factors stimulating excision from *Streptomyces scabiei* chromosome of the toxicogenic region responsible for pathogenicity. Mol Plant Pathol 17:501–509. https://doi.org/10.1111/mpp.12296
19. Joshi M, Rong X, Moll S, Kers J, Franco C, Loria R. 2007. *Streptomyces turgidiscabies* secretes a novel virulence protein, Nec1, which facilitates infection . Mol Plant Microbe Interact 20:599–608. https://doi.org/10.1094/MPMI-20-6-0599
20. Seipke RF, Loria R. 2008. *Streptomyces scabies* 87-22 possesses a functional tomatinase. J Bacteriol 190:7684–7692. https://doi.org/10.1128/JB.01010-08
21. Huguet-Tapia JC, Badger JH, Loria R, Pettis GS. 2011. *Streptomyces turgidiscabies* Car8 contains a modular pathogenicity island that shares virulence genes with other actinobacterial plant pathogens. Plasmid 65:118–124. https://doi.org/10.1016/j.plasmid.2010.11.002
22. Clark CA, Watson B. 1983. Susceptibility of weed species of Convolvulaceae to root-infecting pathogens of Sweetpotato. Plant Dis 67:907–909. https://doi.org/10.1094/PD-67-907
23. Clark CA, Moyer JW. 1988. Compendium of sweet potato diseases. The American Phytopathological Society, St. Paul, MN.
24. King RR, Lawrence CH, Calhoun LA, Ristaino JB. 1994. Isolation and characterization of thaxtomin-type phytotoxins associated with *Streptomyces ipomoeae*. J Agric Food Chem 42:1791–1794. https://doi.org/10.1021/jf00044a042
25. Guan D, Grau BL, Clark CA, Taylor CM, Loria R, Pettis GS. 2012. Evidence that thaxtomin C is a pathogenicity determinant of *Streptomyces ipomoeae,* the causative agent of *Streptomyces* soil rot disease of sweet potato. Mol Plant Microbe Interact 25:393–401. https://doi.org/10.1094/MPMI-03-11-0073
26. Clark CA, Chen C, Ward-Rainey N, Pettis GS. 1998. Diversity within *Streptomyces ipomoeae* based on inhibitory interactions, rep-PCR, and plasmid profiles. Phytopathology 88:1179–1186. https://doi.org/10.1094/PHYTO.1998.88.11.1179
27. Zhang X, Clark CA, Pettis GS. 2003. Interstrain inhibition in the sweet potato pathogen *Streptomyces ipomoeae*: purification and characterization of a highly specific bacteriocin and cloning of its structural gene . Appl Environ Microbiol 69:2201–2208. https://doi.org/10.1128/AEM.69.4.2201-2208.2003
28. Huguet-Tapia JC, Lefebure T, Badger JH, Guan D, Pettis GS, Stanhope MJ, Loria R. 2016. Genome content and phylogenomics reveal both ancestral and lateral evolutionary pathways in plant-pathogenic *Streptomyces* species. Appl Environ Microbiol 82:2146–2155. https://doi.org/10.1128/AEM.03504-15
29. Person LH, Martin MJ. 1940. Soil rot of sweet potatoes in Louisiana. Phytopathology 30:913–926.
30. Huguet-Tapia JC, Loria R. 2012. Draft genome sequence of *Streptomyces acidiscabies* 84-104, an emergent plant pathogen. J Bacteriol 194:1847. https://doi.org/10.1128/JB.06767-11
31. Tomihama T, Nishi Y, Sakai M, Ikenaga M, Okubo T, Ikeda S. 2016. Draft genome sequences of *Streptomyces scabiei* S58, *Streptomyces turgidiscabies* T45, and *Streptomyces* acidiscabies a10, the pathogens of potato

common scab isolated in Japan. Genome Announc 4:e00062-16. https://doi.org/10.1128/genomeA.00062-16
32. Ju K-S, Gao J, Doroghazi JR, Wang K-KA, Thibodeaux CJ, Li S, Metzger E, Fudala J, Su J, Zhang JK, Lee J, Cioni JP, Evans BS, Hirota R, Labeda DP, van der Donk WA, Metcalf WW. 2015. Discovery of phosphonic acid natural products by mining the genomes of 10,000 actinomycetes. Proc Natl Acad Sci U S A 112:12175–12180. https://doi.org/10.1073/pnas.1500873112
33. Ikeda H, Ishikawa J, Hanamoto A, Shinose M, Kikuchi H, Shiba T, Sakaki Y, Hattori M, Omura S. 2003. Complete genome sequence and comparative analysis of the industrial microorganism *Streptomyces avermitilis*. Nat Biotechnol 21:526–531. https://doi.org/10.1038/nbt820
34. Wang XJ, Yan YJ, Zhang B, An J, Wang JJ, Tian J, Jiang L, Chen YH, Huang SX, Yin M, Zhang J, Gao AL, Liu CX, Zhu ZX, Xiang WS. 2010. Genome sequence of the milbemycin-producing bacterium *Streptomyces bingchenggensis*. J Bacteriol 192:4526–4527. https://doi.org/10.1128/JB.00596-10
35. Bentley SD, Chater KF, Cerdeño-Tárraga A-M, Challis GL, Thomson NR, James KD, Harris DE, Quail MA, Kieser H, Harper D, Bateman A, Brown S, Chandra G, Chen CW, Collins M, Cronin A, Fraser A, Goble A, Hidalgo J, Hornsby T, Howarth S, Huang C-H, Kieser T, Larke L, Murphy L, Oliver K, O'Neil S, Rabbinowitsch E, Rajandream M-A, Rutherford K, Rutter S, Seeger K, Saunders D, Sharp S, Squares R, Squares S, Taylor K, Warren T, Wietzorrek A, Woodward J, Barrell BG, Parkhill J, Hopwood DA. 2002. Complete genome sequence of the model actinomycete *Streptomyces coelicolor* A3(2). Nature 417:141–147. https://doi.org/10.1038/417141a
36. Labeda DP. 2016. Taxonomic evaluation of putative *Streptomyces scabiei* strains held in the ARS culture collection (NRRL) using multi-locus sequence analysis. Antonie van Leeuwenhoek 109:349–356. https://doi.org/10.1007/s10482-015-0637-6
37. Ohnishi Y, Ishikawa J, Hara H, Suzuki H, Ikenoya M, Ikeda H, Yamashita A, Hattori M, Horinouchi S. 2008. Genome sequence of the streptomycin-producing microorganism *Streptomyces griseus* IFO 13350 . J Bacteriol 190:4050–4060. https://doi.org/10.1128/JB.00204-08
38. Rückert C, Albersmeier A, Busche T, Jaenicke S, Winkler A, Friðjónsson ÓH, Hreggviðsson GÓ, Lambert C, Badcock D, Bernaerts K, Anne J, Economou A, Kalinowski J. 2015. Complete genome sequence of *Streptomyces lividans* TK24. J Biotechnol 199:21–22. https://doi.org/10.1016/j.jbiotec.2015.02.004
39. Bignell DRD, Huguet-Tapia JC, Joshi MV, Pettis GS, Loria R. 2010. What does it take to be a plant pathogen: genomic insights from *Streptomyces* species. Antonie Van Leeuwenhoek 98:179–194. https://doi.org/10.1007/s10482-010-9429-1
40. Bignell DRD, Seipke RF, Huguet-Tapia JC, Chambers AH, Parry RJ, Loria R. 2010. *Streptomyces scabies* 87-22 contains a coronafacic acid-like biosynthetic cluster that contributes to plant-microbe interactions. Mol Plant Microbe Interact 23:161–175. https://doi.org/10.1094/MPMI-23-2-0161
41. Takasuka TE, Acheson JF, Bianchetti CM, Prom BM, Bergeman LF, Book AJ, Currie CR, Fox BG. 2014. Biochemical properties and atomic resolution structure of a proteolytically processed beta-mannanase from cellulolytic *Streptomyces* sp SirexAA-E. PLoS One 9:e94166. https://doi.org/10.1371/journal.pone.0094166
42. Pullan ST, Chandra G, Bibb MJ, Merrick M. 2011. Genome-wide analysis of the role of GlnR in *Streptomyces venezuelae* provides new insights into global nitrogen regulation in actinomycetes. BMC Genomics 12:175. https://doi.org/10.1186/1471-2164-12-175
43. Oliynyk M, Samborskyy M, Lester JB, Mironenko T, Scott N, Dickens S, Haydock SF, Leadlay PF. 2007. Complete genome sequence of the erythromycin-producing bacterium *Saccharopolyspora erythraea* NRRL23338. Nat Biotechnol 25:447–453. https://doi.org/10.1038/nbt1297
44. Goris J, Konstantinidis KT, Klappenbach JA, Coenye T, Vandamme P, Tiedje JM. 2007. DNA-DNA hybridization values and their relationship to whole-genome sequence similarities. Int J Syst Evol Microbiol 57:81–91. https://doi.org/10.1099/ijs.0.64483-0
45. Beyazova M, Lechevalier MP. 1993. Taxonomic utility of restriction endonuclease fingerprinting of large DNA fragments from *Streptomyces* strains. Inter J of Sys Bact 43:674–682. https://doi.org/10.1099/00207713-43-4-674
46. Labeda DP, Lyons AJ. 1992. DNA relatedness among strains of the sweet potato pathogen *Streptomyces ipomoea* (Person and Martin 1940) Waksman and Henrici 1948. Appl Environ Microbiol 58:532–535. https://doi.org/10.1128/aem.58.2.532-535.1992
47. Carver T, Harris SR, Berriman M, Parkhill J, McQuillan JA. 2012. Artemis: an integrated platform for visualization and analysis of high-throughput sequence-based experimental data. Bioinformatics 28:464–469. https://doi.org/10.1093/bioinformatics/btr703
48. Esposito D, Scocca JJ. 1997. The integrase family of tyrosine recombinases: evolution of a conserved active site domain. Nucleic Acids Res 25:3605–3614. https://doi.org/10.1093/nar/25.18.3605
49. Huguet-Tapia JC, Bignell DRD, Loria R, Vinatzer BA. 2014. Characterization of the integration and modular excision of the integrative conjugative element PAISt in *Streptomyces turgidiscabies* Car8. PLoS ONE 9:e99345. https://doi.org/10.1371/journal.pone.0099345
50. Pettis GS. 2018. Spreading the news about the novel conjugation mechanism in *Streptomyces* bacteria. Environ Microbiol Rep 10:503–510. https://doi.org/10.1111/1758-2229.12659
51. Thoma L, Muth G. 2016. Conjugative DNA-transfer in *Streptomyces*, a mycelial organism. Plasmid 87–88:1–9. https://doi.org/10.1016/j.plasmid.2016.09.004
52. Bellanger X, Payot S, Leblond-Bourget N, Guédon G. 2014. Conjugative and mobilizable genomic islands in bacteria: evolution and diversity. FEMS Microbiol Rev 38:720–760. https://doi.org/10.1111/1574-6976.12058
53. Liu M, Li X, Xie Y, Bi D, Sun J, Li J, Tai C, Deng Z, Ou HY. 2019. ICEberg 2.0: an updated database of bacterial integrative and conjugative elements. Nucleic Acids Res 47:D660–D665. https://doi.org/10.1093/nar/gky1123
54. Emms DM, Kelly S. 2015. OrthoFinder: solving fundamental biases in whole genome comparisons dramatically improves orthogroup inference accuracy. Genome Biol 16:157. https://doi.org/10.1186/s13059-015-0721-2
55. Alvarez-Carreño C, Alva V, Becerra A, Lazcano A. 2018. Structure, function and evolution of the hemerythrin-like domain superfamily. Protein Sci 27:848–860. https://doi.org/10.1002/pro.3374
56. Johnson EG, Sparks JP, Dzikovski B, Crane BR, Gibson DM, Loria R. 2008. Plant-pathogenic *Streptomyces* species produce nitric oxide synthase-derived nitric oxide in response to host signals. Chem Biol 15:43–50. https://doi.org/10.1016/j.chembiol.2007.11.014
57. Rademacher C, Masepohl B. 2012. Copper-responsive gene regulation in bacteria. Microbiology 158:2451–2464. https://doi.org/10.1099/mic.0.058487-0
58. González-Quiñónez N, Corte-Rodríguez M, Álvarez-Fernández-García R, Rioseras B, López-García MT, Fernández-García G, Montes-Bayón M, Manteca A, Yagüe P. 2019. Cytosolic copper is a major modulator of germination, development and secondary metabolism in *Streptomyces coelicolor*. Sci Rep 9:4214. https://doi.org/10.1038/s41598-019-40876-0
59. Vrancken K, Van Mellaert L, Anné J. 2008. Characterization of the *Streptomyces lividans* PspA response . J Bacteriol 190:3475–3481. https://doi.org/10.1128/JB.01966-07
60. Tran NT, Huang X, Hong HJ, Bush MJ, Chandra G, Pinto D, Bibb MJ, Hutchings MI, Mascher T, Buttner MJ. 2019. Defining the regulon of genes controlled by sigma(E), a key regulator of the cell envelope stress response in *Streptomyces coelicolor*. Mol Microbiol 112:461–481. https://doi.org/10.1111/mmi.14250
61. Lautru S, Oves-Costales D, Pernodet JL, Challis GL. 2007. MbtH-like protein-mediated cross-talk between non-ribosomal peptide antibiotic and siderophore biosynthetic pathways in *Streptomyces coelicolor* M145. Microbiology (Reading) 153:1405–1412. https://doi.org/10.1099/mic.0.2006/003145-0
62. Wolpert M, Gust B, Kammerer B, Heide L. 2007. Effects of deletions of *mbtH*-like genes on clorobiocin biosynthesis in *Streptomyces coelicolor*. Microbiology (Reading) 153:1413–1423. https://doi.org/10.1099/mic.0.2006/002998-0
63. Guan D. 2011. Insights into the molecular mechanism of *Streptomyces ipomoeae* pathogenesis: thaxtomin C biosynthesis and regulation. Ph.D. Louisiana State University, Baton Rouge, LA.
64. Blin K, Shaw S, Steinke K, Villebro R, Ziemert N, Lee SY, Medema MH, Weber T. 2019. antiSMASH 5.0: updates to the secondary metabolite genome mining pipeline. Nucleic Acids Res 47:W81–W87. https://doi.org/10.1093/nar/gkz310

65. Baerson SR, Schröder J, Cook D, Rimando AM, Pan Z, Dayan FE, Noonan BP, Duke SO. 2010. Alkylresorcinol biosynthesis in plants: new insights from an ancient enzyme family? Plant Signal Behav 5:1286–1289. https://doi.org/10.4161/psb.5.10.13062
66. Funabashi M, Funa N, Horinouchi S. 2008. Phenolic lipids synthesized by type III polyketide synthase confer penicillin resistance on *Streptomyces griseus*. J Biol Chem 283:13983–13991. https://doi.org/10.1074/jbc.M710461200
67. Omura S, Tomoda H, Xu QM, Takahashi Y, Iwai Y. 1986. Triacsins, new inhibitors of acyl-CoA synthetase produced by *Streptomyces* sp. J Antibiot (Tokyo) 39:1211–1218. https://doi.org/10.7164/antibiotics.39.1211
68. Tomoda H, Igarashi K, Omura S. 1987. Inhibition of acyl-CoA synthetase by triacsins. Biochim Biophys Acta 921:595–598.
69. Zimina M, Babich O, Prosekov A, Sukhikh S, Ivanova S, Shevchenko M, Noskova S. 2020. Overview of global trends in classification, methods of preparation and application of bacteriocins. Antibiotics (Basel) 9:553. https://doi.org/10.3390/antibiotics9090553
70. Bertelli C, Laird MR, Williams KP, Lau BY, Hoad G, Winsor GL, Brinkman FS, Simon Fraser University Research Computing Group. 2017. Islandviewer 4: expanded prediction of Genomic Islands for larger-scale Datasets. Nucleic Acids Res 45:W30–W35. https://doi.org/10.1093/nar/gkx343
71. Vernikos GS, Parkhill J. 2006. Interpolated variable order motifs for identification of horizontally acquired DNA: revisiting the *Salmonella* pathogenicity islands. Bioinformatics 22:2196–2203. https://doi.org/10.1093/bioinformatics/btl369
72. Moyer JW, Campbell CL, Echandi E, Collins WW. 1984. Improved methodology for evaluating resistance in sweet potato to Streptomyces Ipomoea. Phytopathology 74:494–497. https://doi.org/10.1094/Phyto-74-494
73. Li W, Wu J, Tao W, Zhao C, Wang Y, He X, Chandra G, Zhou X, Deng Z, Chater KF, Tao M. 2007. A genetic and bioinformatic analysis of *Streptomyces coelicolor* genes containing TTA codons, possible targets for regulation by a developmentally significant tRNA. FEMS Microbiol Lett 266:20–28. https://doi.org/10.1111/j.1574-6968.2006.00494.x
74. Myers EW, Sutton GG, Delcher AL, Dew IM, Fasulo DP, Flanigan MJ, Kravitz SA, Mobarry CM, Reinert KH, Remington KA, et al. 2000. A whole-genome assembly of *Drosophila*. Science 287:2196–2204. https://doi.org/10.1126/science.287.5461.2196
75. Delcher AL, Harmon D, Kasif S, White O, Salzberg SL. 1999. Improved microbial gene identification with GLIMMER. Nucleic Acids Res 27:4636–4641. https://doi.org/10.1093/nar/27.23.4636
76. Seemann T. 2014. Prokka: rapid prokaryotic genome annotation. Bioinformatics 30:2068–2069. https://doi.org/10.1093/bioinformatics/btu153
77. Assefa S, Keane TM, Otto TD, Newbold C, Berriman M. 2009. ABACAS: algorithm-based automatic contiguation of assembled sequences. Bioinformatics 25:1968–1969. https://doi.org/10.1093/bioinformatics/btp347
78. Emms DM, Kelly S. 2019. OrthoFinder: phylogenetic orthology inference for comparative genomics. Genome Biol 20:238. https://doi.org/10.1186/s13059-019-1832-y
79. Bierman M, Logan R, O'Brien K, Seno ET, Rao RN, Schoner BE. 1992. Plasmid cloning vectors for the conjugal transfer of DNA from *Escherichia coli* to *Streptomyces* spp. Gene 116:43–49. https://doi.org/10.1016/0378-1119(92)90627-2
80. Guan D, Pettis GS. 2009. Intergeneric conjugal gene transfer from *Escherichia coli* to the sweet potato pathogen *Streptomyces ipomoeae*. Lett Appl Microbiol 49:67–72. https://doi.org/10.1111/j.1472-765X.2009.02619.x
81. Pettis GS, Cohen SN. 1994. Transfer of the pIJ101 plasmid in *Streptomyces lividans* requires a *cis*-acting function dispensable for chromosomal gene transfer. Mol Microbiol 13:955–964. https://doi.org/10.1111/j.1365-2958.1994.tb00487.x